SLAC-PUB-2405
LBL-9851
September 1979
(T/E)

# RESULTS FROM THE MARK II DETECTOR AT SPEAR*

SLAC-LBL Collaboration[1]

Presented by Vera Lüth
Stanford Linear Accelerator Center
Stanford University, Stanford, California 94305

## Summary

Recent results from the Mark II include measurements of the $\rho^{\pm}\nu$ decay of the $\tau^{\pm}$-lepton, two-photon production of the $\eta'(958)$ meson, charmed meson decays and the first observation of charmed baryons in $e^+e^-$ annihilation.

## Introduction

At the time of the last Photon-Lepton Conference in Hamburg the SLAC-LBL collaboration abandoned the solenoidal magnetic detector at SPEAR after four years of operation. It was replaced by Mark II, a detector quite similar in dimensions and layout, but with considerably improved solid angle, resolution and particle identification. This summer, Mark II is being installed at PEP, the new high energy $e^+e^-$ storage ring at SLAC, that is expected to provide beams early next year.

Since the energy range between 3 GeV and 7.5 GeV had already been exploited for several years by experiments at SPEAR and DORIS, the Mark II program was aimed at questions that had not been investigated in sufficient detail due to low rates and considerable background. Data were recorded at the $\psi(3095)$, $\psi(3684)$, and $\psi(3770)$ resonances, at 3.67 GeV, 5.20 GeV, 6.5 GeV, and 7.4 GeV. Furthermore, a systematic exploration of the total hadron production in the range from 3.7 GeV to 6.0 GeV was made by increasing the cm energy in steps of 6-20 MeV and recording 100-300 $\mu^+\mu^-$ pairs per point. Preliminary results on radiative decays of the $\psi(3095)$ and the $\psi(3684)$ have been reported recently,[2,3] results on the total hadronic cross section are forthcoming. Following a description of the Mark II detector, the following topics will be discussed here:

(1) the decay $\tau^{\pm} \to \rho^{\pm}\nu_{\tau}$
(2) the $\gamma\gamma$ process $e^+e^- \to e^+e^-\,\eta'(958)$
(3) the $\psi(3770)$ resonance
(4) decays of the D-mesons
(5) search for the $F^{\pm}$ meson
(6) inclusive baryon production
(7) evidence for charmed baryon production.

A considerable fraction of the results presented here has not been published and is to be regarded as preliminary.

## Apparatus

The Mark II detector,[4] schematically shown in Fig. 1, has been in operation at the SLAC $e^+e^-$ colliding beam facility, SPEAR, since the end of 1977. It was designed to measure charged particles and photons with good resolution and efficiency, to identify electrons and muons with low hadron contamination, and to separate charged pions from kaons and protons over a wide momentum range. The performance of the principal components of the detector can be summarized as follows:

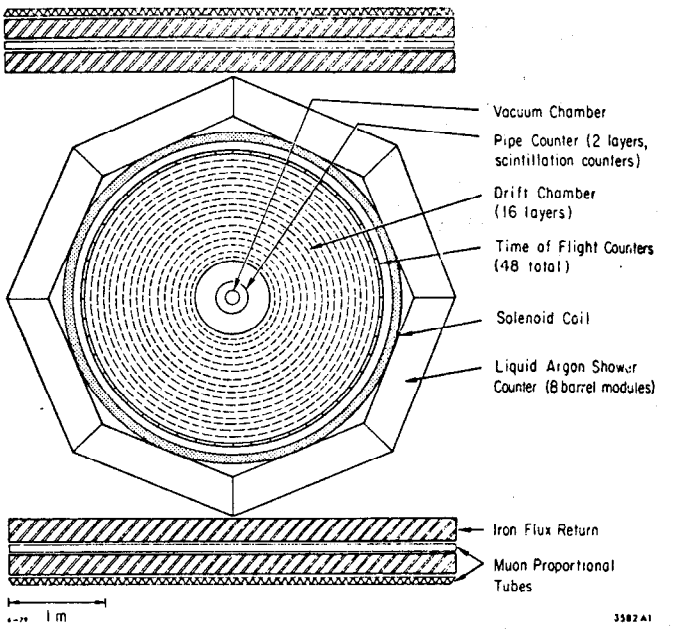


Fig. 1. End view of the SLAC-LBL Mark II detector.

(1) The drift chambers[5] measure the azimuthal coordinates of charged particle tracks to an average accuracy of 200 μm at each of the 6 axial layers, the polar coordinates are determined from the 10 stereo layers stretched at $\pm 3^{\circ}$ to the beam axis. For tracks constrained to originate from the beam, the rms momentum resolution can be parameterized as $\delta p/p = [(0.005p)^2 + (0.0145)^2]^{\frac{1}{2}}$, where the momentum p is measured in GeV/c. The first term is the contribution from the measurement error, the second term gives the multiple scattering error. The tracking efficiency is greater than 95% for momenta above 100 MeV/c over a solid angle of 75% of $4\pi$.

(2) The time-of-flight system (TOF) has a rms resolution of 300 ps for charged hadrons, leading to a separation by one standard deviation between electrons and pions at 300 MeV/c, between pion and kaons at 1.35 GeV/c, and between kaons and protons at 2.0 GeV/c. In practice, the following technique is applied to identify hadrons. Each charged particle is assigned three weights proportional to the probabilities that the measured TOF is compatible with a $\pi$, K or proton. These weights are determined from the measured momentum and time-of-flight assuming a Gaussian distribution with a standard deviation of 0.3 ns. The relative $\pi$-K-p weights are normalized so that their sum is unity, and a hadron is identified as a proton or kaon if the respective weight exceeds 0.5, otherwise it is called a pion.

* Work supported primarily by the Department of Energy under contracts DE-AC03-76SF00515 and W-7405-ENG-48.

(Invited talk presented at the 1979 International Symposium on Lepton and Photon Interaction at High Energy, Batavia, Illinois, August 23-29, 1979.)

(3) The lead-liquid argon shower counters (LA)[6] surrounding the inner detector contain about 14 radiation lengths of lead and argon with read-out strips parallel, perpendicular and at 45° to the beam, giving an angular resolution of 8 mrad in azimuth and polar angle. The energy resolution for electrons and photons above 500 MeV is $\delta E/E = 0.11/\sqrt{E}$, where E is the energy in GeV. The resolution degrades slightly at lower energies due to energy loss in the coil material (1.36 radiation lengths). The photon detection efficiency of the LA barrel modules has been measured in the decays $\psi \to \pi^+\pi^-\pi^0$ and $\psi \to \pi^+\pi^+\pi^-\pi^-\pi^0$, where one observed $\gamma$ is used to determine the position of the other $\gamma$ by a 2C kinematical fit. The result, shown in Fig. 2a, is in good agreement with a Monte Carlo calculation simulating the electromagnetic shower development.[7] This efficiency, combined with the geometric acceptance of the LA system (64%) and the known branching ratios to photons, then translates into detection efficiencies for $\pi^0$ and $\eta^0$ (Fig. 2b).

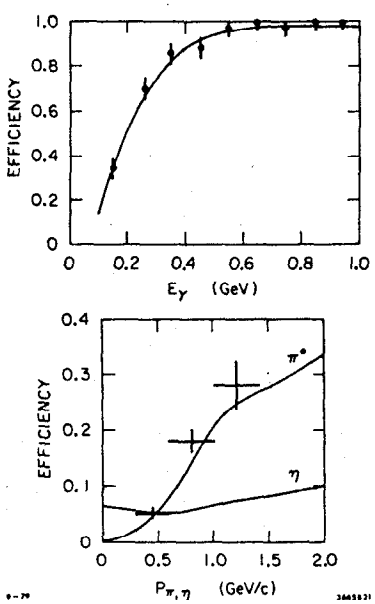


Fig. 2. Efficiency for detecting (a) photons (not including geometrical acceptance) and (b) $\pi^0$ and $\eta^0$ via their $\gamma\gamma$ decay. The curves represent Monte Carlo predictions.

(4) Muons are detected in two layers of proportional tubes interleaved with hadron absorbers on top and bottom as well as on the sides of the detector. The first layers have a threshold momentum of 700 MeV/c, the second of 1 GeV/c. The detector efficiency for momenta above threshold is ≥98%, the probability that a pion is misidentified as a μ is 4% at 700 MeV/c, 11% at 900 MeV/c and 2% above 1 GeV/c.

(5) Above 300 MeV/c electrons are separated from hadrons by a series of cuts in the total energy deposition and the transverse and longitudinal shower development. The probability that a pion is misidentified as an electron decreases with energy, it is 7% below 500 MeV/c, 4% at 600 MeV/c, and 2% at 800 MeV/c.

(6) The standard trigger[8] requires at least one charged particle to be within the central 75% of the solid angle and a second charged track to be within 85% of the 4π sterad. Up to now, totally neutral final states have not been recorded.

(7) The luminosity is monitored by two pairs of small counters measuring Bhabha scattering at 25 mrad, it is checked against wide angle Bhabha events in the central detector.

The data analysis constructs tracks and vertices from the raw data and selects four classes of events corresponding to the reactions $e^+e^- \to$ hadrons, $e^+e^- \to \tau^+\tau^-$, $e^+e^- \to \mu^+\mu^-$, and $e^+e^- \to e^+e^-$. A hadronic event is required to have 3 or more tracks or 2 tracks that are acoplanar to the beam by more than 20°. Background due to beam-gas interaction is measured from longitudinal distribution of the reconstructed vertices.

## Measurement of the Branching Fraction for $\tau^\pm \to \rho^\pm\nu$

The existence of a new charged heavy lepton, $\tau^\pm$, was first suggested[9] to explain the presence of events in which the only detected particles were an electron and a muon of opposite charge. The experimental evidence accumulated since that time strongly supports this interpretation and there now exists a coherent picture of the τ as a sequential heavy lepton with a light or massless neutrino which couples via the conventional V-A weak current.[10] In addition, there are several precise measurements of the τ mass and branching ratios for leptonic and some hadronic decays.[11] The Mark II group has measured the branching ratio for the decay $\tau^- \to \rho^-\nu_\tau$.[12] This decay[13] involves only the vector part of the weak hadronic current. Comparison of this measurement with theoretical predictions, based on the coupling of the ρ to the electromagnetic current, constitutes a test of the validity of the conserved vector current hypothesis (CVC).

The analysis is aimed at events of the following topology:

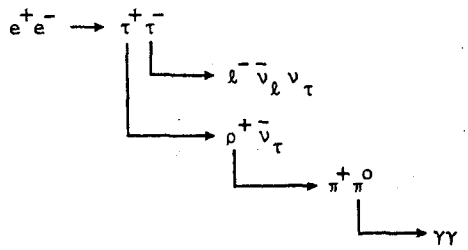


which results in two charged particles and two photons from $\pi^0$ decay in the detector. $\ell^-$ represents either an electron or a muon which helps to provide a clean signature for τ-pair production. Selected events have two oppositely charged tracks, one a pion, the other a muon or an electron, acoplanar to the beam by at least 20°, and two photons in the LA shower counters with $E_\gamma > 100$ MeV. For events with a two photon invariant mass (Fig. 3) compatible with a $\pi^0$, the photon energies are adjusted by a one constraint fit. The resulting mass spectrum of the $\pi^\pm\pi^0$ system is shown in Fig. 4. The data can be fit to the sum of a smooth background and a Breit-Wigner resonance. The fit yields a mass $M = 0.770 \pm 0.020$ GeV/c² and a width $\Gamma = 0.194 \pm 0.030$ GeV/c², well compatible with the $\rho^\pm$ resonance parameters. There are 85 events in the peak, $64\rho^\pm e^\mp$ and $21\rho^\pm\mu^\mp$. The energy spectrum of the $85\rho^\pm$ candidates is shown in Fig. 5.

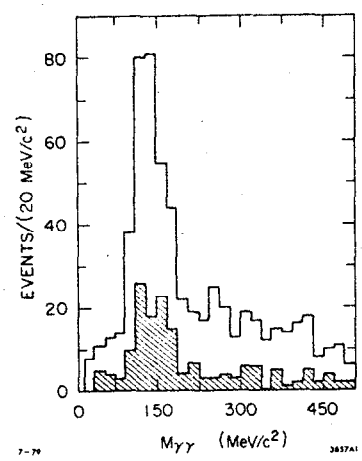


Fig. 3. Two photon invariant mass spectrum for acoplanar two-prongs with two photons. Events with one identified lepton, $e^{\pm}$ or $\mu^{\pm}$, are shaded.

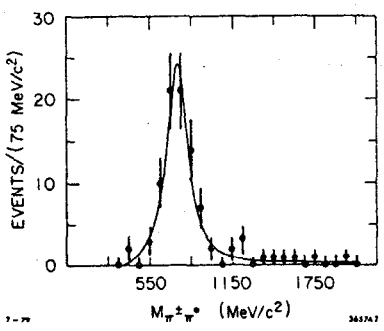


Fig. 4. $\pi^{\pm}\pi^{0}$ invariant mass spectrum in candidate events for the decay $\tau \to \rho\nu_{\tau}$.

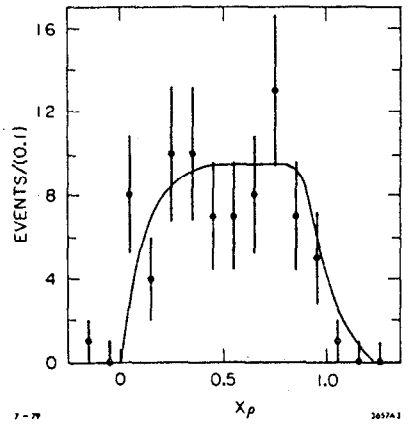


Fig. 5. Distribution $x_{\rho} = (E_{\rho} - E_{min})/(E_{max} - E_{min})$ for the 85 candidates for $\tau \to \rho\nu_{\tau}$.

The variable $x_{\rho}$ is defined as $x_{\rho} = (E - E_{min})/(E_{max} - E_{min})$, where $E_{\rho}$ is the energy of the $\rho^{\pm}$, $E_{min}$ and $E_{max}$ are the minimum and maximum energies for a $\rho^{\pm}$ produced in a $\tau$ decay at a given beam energy. The data are in good agreement with a Monte Carlo simulation for the decay $\tau \to \rho^{\pm}\nu_{\tau}$.

Background studies indicate that multihadrons contribute only 4 events to the sample. The remaining 81 events are genuine $\tau$ decays, of which we estimate contributions from $\tau \to A_1\nu$ and $\tau \to 4\pi\nu$ to amount to $8.3\rho^{\pm}e^{\mp}$ and $2.6\rho^{\pm}\mu^{\mp}$ events. The efficiencies for detecting $\rho e$ and $\rho\mu$ events have been found by Monte Carlo to be $\varepsilon_{\rho e} = 6.4\%$ and $\varepsilon_{\rho\mu} = 2.7\%$. In addition, 12.7% of all events are lost due to spurious photons.

In order to extract the $\tau^- \to \rho^-\nu_{\tau}$ branching ratio from the $\rho^{\mp}\ell^{\pm}$ events, we need to know $B(\tau^- \to \ell^-\bar{\nu}_e\nu_{\tau})$. There are 95 $\mu e$ events in the same data sample, i.e., events with an electron, a muon, and no detected photon. The detection efficiency for these $\tau$ decays is $\varepsilon_{e\mu} = 12.1\%$, including the loss due to spurious photons. From the corrected number of events and the total number of $\tau^+\tau^-$ pairs produced we obtain

$$B(\tau^- \to \rho^-\nu_{\tau})\, B(\tau^+ \to e^+\bar{\nu}_{\tau}\nu_e) = 0.042 \pm 0.009 \quad ,$$

$$B(\tau^- \to \rho^-\nu_{\tau})\, B(\tau^+ \to \mu^+\bar{\nu}_{\tau}\nu_{\mu}) = 0.033 \pm 0.010 \quad ,$$

and

$$\sqrt{B(\tau^- \to e^-\nu_{\tau}\bar{\nu}_e) \cdot B(\tau^+ \to \mu^+\bar{\nu}_{\tau}\nu_{\mu})} = 0.185 \pm 0.015 \, .$$

The errors quoted are based on the statistics of the uncorrected events and the statistical errors of the corrections and Monte Carlo calculations. In addition systematic errors have been included to account for uncertainties in the luminosity, the lepton identification and radiative corrections in the initial state.

If we assume $\mu$-e universality in $\tau$-decay, we obtain

$$B(\tau^- \to \rho^-\nu_{\tau}) = (20.5 \pm 4.1)\%$$

$$B(\tau^- \to e^-\bar{\nu}_e\nu_{\tau}) = (18.5 \pm 1.5)\%$$

and

$$\frac{B(\tau^- \to \rho^-\nu_{\tau})}{B(\tau^- \to e^-\bar{\nu}_e\nu_{\tau})} = 1.11 \pm 0.24$$

This result is in good agreement with a prediction[14] of 1.2 based on the CVC hypothesis and a measurement of $e^+e^- \to \rho^0$. The result is also in agreement with a measurement by the DASP group,[15] yielding $B(\tau \to \rho\nu) = (24 \pm 9)\%$. The measurements presented here are based on one quarter of the total data now available. A more thorough study of the leptonic decays $\tau^{\pm} \to \ell^{\pm}\nu_e\nu_{\tau}$ is underway. Of particular interest is the decay $\tau^{\pm} \to A_1^{\pm}\nu_{\tau}$, since it might help to establish the $A_1$ as a resonance. A preliminary measurement of the branching ratio for $\tau \to \pi\nu$ has been obtained, $B(\tau \to \pi\nu) = (10.7 \pm 2.1)\%$. A more detailed study of this decay will be used to set an upper limit on the mass of $\nu_{\tau}$.

## Evidence for Hadron Production by Two-Photon Annihilation

Though the production of leptons and hadrons by two-photon interaction in colliding beam experiments has generally been considered a background to the dominant one-photon annihilation process, its importance was pointed out by F. E. Low and others[16] several years ago. The basic diagram in Fig. 6 shows the annihilation of two nearly on-shell photons producing hadrons at small angles to the beam. The

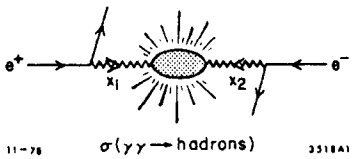


Fig. 6. Two photon annihilation into hadrons in $e^+e^-$ collisions.

hadron system has charge conjugation $C = +1$ and angular momentum $J = 0, 2$. Resonances like $\eta$, $\eta'$, $\eta_c$, $f^o$ and $A_2$ can be produced directly; their production cross sections are of fourth order in $\alpha$ but increase logarithmically with the beam energy E,

$$\sigma_M \sim (2J+1)\, M^{-3}\, \Gamma_{M\to\gamma\gamma}\left(\ln\frac{E}{m_e} - \frac{1}{2}\right)^2 f\left(\frac{M}{2E}\right)$$

where M is the mass of the state, J its spin, and f gives the effective $\gamma\gamma$ luminosity for a mass M at a beam energy E.

The Mark II group has recently published evidence for $\eta'(958)$ production[17] in the reaction

$$e^+e^- \;\to\; e^+e^-\,\eta'(958)$$

where the $\eta'$ is detected via its decay to $\rho^o\gamma$. The final state $e^+$ and $e^-$ are not detected. In the meantime, the high energy data sample has been doubled and the analysis has been extended to include other resonances. In the following, only details of the $\eta'$ measurement are given.

The events are selected by topology; two oppositely charged pions coming from the interaction region, and a single photon with an energy $E_\gamma > 180$ MeV in the LA module. This requirement reduces background from fake photons. Background from one-photon annihilation is reduced by requiring that the transverse momentum of the $\pi\pi\gamma$ state be less than 250 MeV/c and that the dipion system and $\gamma$ be coplanar to within 0.35 rad with respect to the beam. The contribution from lepton or hadron pairs produced in two-photon interactions combined with fake photons is suppressed by requiring the $\pi^+\pi^-$ pair to have a transverse momentum exceeding 50 MeV/c and an acoplanarity angle of more than 0.05 rad.

The $\pi^+\pi^-\gamma$ mass distribution for the remaining events, given in Fig. 7, shows a clear peak at the $\eta'$ mass. The resolution is dominated by the photon energy measurement. No cut has been made on the $\pi^+\pi^-$ invariant mass, but it has been verified that all events in the $\eta'$ mass region (defined as $0.90 < M_{\pi\pi\gamma} < 1.05$ GeV/$c^2$) are compatible with the formation of $\rho^o$.

The distribution of the transverse momentum $p_\perp$, and the rapidity y are shown in Fig. 8. The $\eta'$ events occur mainly at low $p_\perp$ and their angular distribution is highly peaked in the forward and backward direction. The rapidity distribution is flat within the detector acceptance of about $-0.6 < y < 0.6$. These kinematical features are those expected for $\eta'$ production by two-photon interaction. They are well reproduced by Monte Carlo generated events for the same process.[18] Background from $e^+e^-$ annihilation has been studied using events that pass all the above selection criteria but have additional charged tracks or photons. There is no peak in the $\pi^+\pi^-\gamma$ mass and the $p_\perp$ distribution extends well beyond 200 MeV/c.

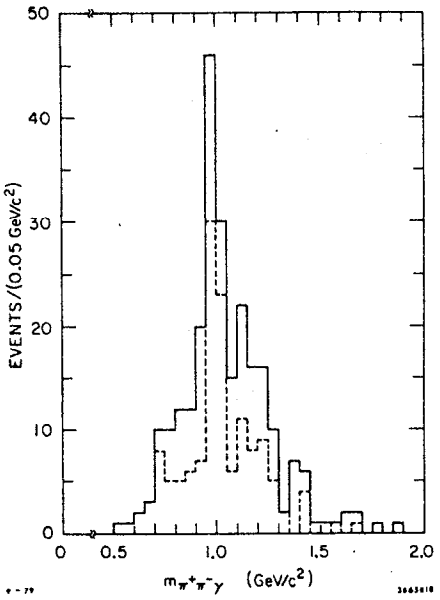


Fig. 7. Invariant $\pi^+\pi^-\gamma$ mass in candidate events for $e^+e^- \to e^+e^-\eta'$. The full histogram contains all events, the high energy data ($E_{cm} = 5.2$ GeV, $6.0 < E_{cm} < 7.4$ GeV) are dashed.

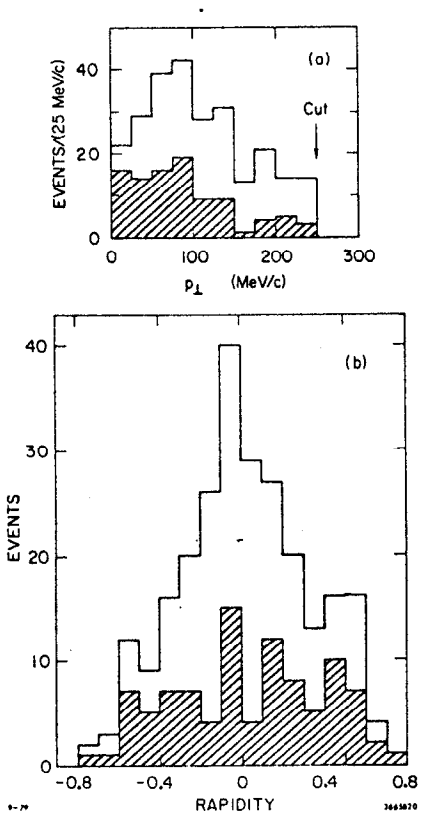


Fig. 8. Distributions for (a) transverse momentum $p_\perp$, and (b) rapidity y for all events and events in the $\eta'$ mass peak (shaded).

The cross section for $\eta'$ production is presented in Fig. 9, using the branching ratio $B(\eta' \to \rho\gamma) = 0.298 \pm 0.017$. From the two-photon cross section for resonance formation, we determine the radiative width of the $\eta'$, $\Gamma_{\gamma\gamma}(\eta') = 5.8 \pm 1.1$ keV. The error is purely statistical, the systematic uncertainties amount to ±25%. Using the measured branching ratio $B(\eta' \to \gamma\gamma) = 0.020 \pm 0.003$, the total width is determined to be $\Gamma_{tot}(\eta') = 290 \pm 91$ keV, in excellent agreement with the only other measurement[19] available.

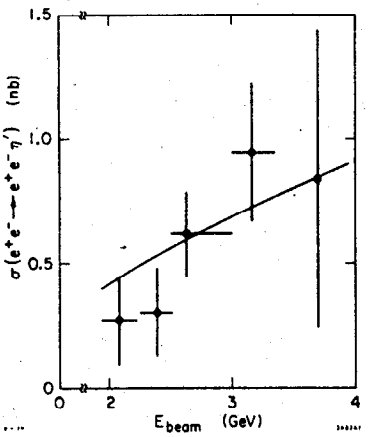


Fig. 9. Cross section for $e^+e^- \to e^+e^-\eta'$ versus the energy of the beam. The errors are statistical only. The curve represents the expected cross section[16] for $\Gamma_{\gamma\gamma} = 6$ keV.

There is considerable interest in the measurement of $\Gamma_{\gamma\gamma}(\eta')$.[20] Models with fractionally charged quarks and a small octet-singlet mixing of pseudoscalars lead under the assumption of equal singlet and octet amplitudes to the prediction $\Gamma_{\gamma\gamma}(\eta') \simeq 6$ keV. A recent calculation[21] based on vector meson dominance and flavor $SU_3$ symmetry is under the assumption of fractionally charged quarks in agreement with this measurement, while it disagrees for quarks of the Han-Nambu type.

## Charmed Meson Decays

The $\psi(3770)$ resonance,[22,23] roughly 40 MeV/$c^2$ (30 MeV/$c^2$) above the threshold for $D^0\bar{D}^0$ ($D^+D^-$) production but below the threshold for $D\bar{D}^*$ production, represents a source of kinematically well defined and relatively background-free D-mesons. Precise knowledge of the resonance parameters is useful both for comparison with the charmonium model of the $\psi$ states[26] as well as for the determination of the absolute branching ratios for D-mesons. Making use of this convenient source of D-mesons, the Mark II group has performed extensive studies of various decays, exclusively and inclusively, and obtained evidence for the existence of Cabibbo suppressed decays. Unfortunately, a similar resonance enhancement has not been found near the threshold for $F^{\pm}$ meson pair production, and our knowledge of this third charmed meson remains very, very limited.

## The $\psi(3770)$ Resonance

Figure 10a shows R, the ratio of the total cross section for $e^+e^-$ annihilation into hadrons to the theoretical cross section for muon pair production $\sigma_{\mu\mu}$, in the cm energy interval from 3.67 GeV to 3.87

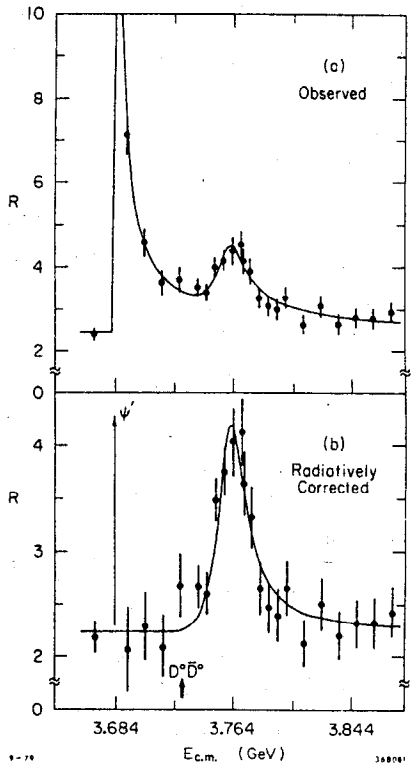


Fig. 10. The ratio of hadron production to μ-pair production near the $\psi(3764)$ resonance (a) observed, and (b) radiatively corrected for the $\psi(3095)$, $\psi(3684)$ and $\psi(3764)$ resonances. The curve represents the fit to the data.

GeV. The $\tau^+\tau^-$ pair production has been subtracted, and radiative corrections have been applied for the continuum, but not for the narrow resonances $\psi(3095)$, $\psi(3684)$, and $\psi(3770)$. The errors shown are purely statistical. Partially obscured by the radiative tail of the $\psi'(3684)$ is an enhancement of about 2 units of R near 3.77 GeV, the $\psi(3770)$ resonance.[22,23] This resonance is only 80 MeV/$c^2$ above the $\psi(3684)$ but substantially broader.

In order to determine the exact mass M, the partial width to electrons $\Gamma_{ee}$, and the total width $\Gamma_{tot}$, the energy dependence of R was fitted to a function that describes the resonance shape and the dominant backgrounds; it includes radiative corrections for the resonance itself, the nearby $\psi(3684)$ and $\psi(3095)$ and the continuum. The resonance is taken to be a non-relativistic p-wave Breit-Wigner with an energy dependent total width $\Gamma_{tot}(E_{cm})$:[24]

$$R(E_{cm}) = \frac{1}{\sigma_{\mu\mu}} \frac{3\pi}{M^2} \frac{\Gamma_{ee}\,\Gamma_{tot}(E_{cm})}{(E_{cm} - M)^2 + \Gamma_{tot}^2(E_{cm})/4}$$

with

$$\Gamma_{tot}(E_{cm}) \propto \frac{p_+^3}{1 + (rp_+)^2} + \frac{p_o^3}{1 + (rp_o)^2}$$

The energy dependence of $\Gamma_{tot}$ accounts for the proximity of the $D\bar{D}$ thresholds and assumes equal production of $D^0\bar{D}^0$ and $D^+D^-$, apart from phase space factors. $p_+$ and

$p_o$ refer to the momentum of the pair-produced $D^+$ and $D^o$, respectively. The width $\Gamma_{tot}(E_{cm})$ is normalized to $\Gamma_{tot} = \Gamma_{tot}(E_{cm} = M)$ at the peak of the resonance. The parameter r is the interaction radius taken to be 2.5 fermi for this analysis. While the resonance parameters are found to be largely insensitive to the exact value of r, it does affect the charged-to-neutral decay fraction in $\Gamma_{tot}$ by at most 5%.

The free parameters of the fit are $\Gamma_{ee}$, $\Gamma_{tot}$, M, and $R_o$. The best fit gives $\chi^2 = 12$ for 17 degrees of freedom. On the basis of this fit and estimates of the systematic uncertainties in the cross section measurement and the background shapes, we find the following parameters of the $\psi(3770)$ resonance:

$$M = 3763.7 \pm 5.1 \text{ MeV}/c^2$$

$$\Gamma_{ee} = 276 \pm 50 \text{ eV}$$

$$\Gamma_{tot} = 23.5 \pm 5.0 \text{ MeV}$$

The error on the mass is dominated by the 0.13% uncertainty in the energy calibration of SPEAR. The Mark II group was able to reproduce the masses of the $\psi$ and $\psi'$ resonances to within 0.5 MeV/$c^2$ of the original values.[25] The total width is most sensitive to the size of the nonresonant background $R_0$. The error on the leptonic width $\Gamma_{ee}$ is caused by uncertainty in the overall normalization and the nonresonant background. Furthermore, $\Gamma_{ee}$ is rather sensitive to the shape of the radiative tail of the $\psi(3684)$ resonance.

The data after removal of the nonresonant background and the radiative tails are presented in Fig. 10b together with the fit. The cross section at the peak is

$$\sigma_{tot}(3.764) = (9.3 \pm 1.4) \text{ nb}$$

After radiative corrections, this corresponds to an enhancement of 1.8 units of R.

The Mark II results presented here deviate somewhat from earlier measurements by the DELCO and LGW (lead glass wall) experiments at SPEAR (Table I). The results agree to within one standard deviation on $\Gamma_{tot}$, the mass we obtain appears 6 MeV/c lower, and the leptonic width measurements basically reflect the difference in the raw data.

The parameters of the $\psi(3770)$ are in excellent agreement with theoretical predictions for the $^3D_1$ state of charmonium.[26] In this framework, the $D_1$ state obtains most of its leptonic width by mixing with the nearby $2^3S_1$ state, the $\psi(3684)$. We obtain a mixing angle of $(20.3 \pm 2.8)^o$.

Table I

Measurements of the $\psi(3770)$ Parameters

| Experiment | Mass (MeV/$c^2$) | $\Gamma_{tot}$(MeV/$c^2$) | $\Gamma_{ee}$(eV/$c^2$) |
|---|---|---|---|
| LGW [22] | 3772 ± 6 | 28 ± 5 | 345 ± 85 |
| DELCO [23] | 3770 ± 6 | 24 ± 5 | 180 ± 60 |
| Mark II | 3764 ± 5 | 24 ± 5 | 276 ± 50 |

D-Meson Decays

The $\psi(3770)$ resonance provides a rich source of kinematically well-defined and relatively background free D-mesons. During 6 weeks of running, the Mark II recorded a sample of 49,000 hadronic events corresponding to a total luminosity of 2850 $nb^{-1}$ at a fixed energy of 3.771 GeV. At this energy the total hadronic cross section corrected for non-resonant contributions amounts to $6.85 \pm 1.42$ nb. In order to obtain the inclusive $D^\pm$ and $D^o$ ($\bar{D}^o$) cross section, we need two assumptions: (1) the $\psi(3770)$ is a state of definite isospin, either 0 or 1; (2) the $\psi(3770)$ decays only to $D\bar{D}$. The rationale for the latter assumption is that the difference in width by two orders of magnitude between the $\psi(3684)$ and the $\psi(3770)$ is due to $D\bar{D}$ decay which is not accessible to the $\psi(3684)$. The isospin assumption leads to equal partial widths to $D^o\bar{D}^o$ and $D^+D^-$, except for phase-space factors. Taking this into account, the inclusive D cross sections at 3.771 GeV are

$$\sigma_{D^+} = 5.9 \pm 1.0 \text{ nb}$$

$$\sigma_{D^o} = 7.8 \pm 1.2 \text{ nb} \quad .$$

The advantage of studying D-mesons at the $\psi(3770)$ resonance is that they are produced in pairs, so that each D-meson has the energy of beam $E_b$. For any combination of kaons and pions which is a candidate for a D-meson decay, like $K^-\pi^+\pi^-$ or $K^-\pi^+$, one requires that the measured energy agrees with $E_b$ to within 50 MeV and then calculates the mass according to

$$M = \sqrt{E_b^2 - p^2} \quad .$$

Since the momentum p is small (~280 MeV/c), M is determined five to ten times more precisely than from a direct measurement. The results of this technique, given in Figs. 11 and 12, show clear signals for five decay modes of the $D^o$ and four decay modes of the $D^\pm$, including the previously unreported modes for $D^o \to \bar{K}^o\pi^o$, $D^+ \to K_s\pi^+\pi^+\pi^-$ and $D^+ \to K_s\pi^\pm\pi^o$. The widths of about 3 MeV/$c^2$ are consistent with the expected experimental resolution. In Table II the branching ratios are presented using the observed number of events and the detection efficiency for each mode combined with the inclusive production cross section for $D^o$ ($\bar{D}^o$) and $D^\pm$. The results are in good agreement with the first measurement by Mark I.[27] The observation of the decay $D^o \to \bar{K}^o\pi^o$ at roughly the same rate as $D^o \to K^-\pi^+$ contradicts the standard theoretical predictions, in particular color suppression.[28] Unfortunately, the test of other predictions by the same concept depends on the rather difficult extraction of relative resonance contributions to three-body decays, like $D^o \to K^-\rho^+$ and $D^o \to \bar{K}^{*o}\pi^o$ in $D^o \to K^-\pi^+\pi^o$. On the other hand, color selection rules can easily be weakened by the emission or absorption of soft gluons.[29]

Cabibbo Suppressed Decays[30]

The standard GIM model[33] favors the $c \leftrightarrow s$ quark coupling over the $c \leftrightarrow d$ coupling as illustrated for $D^o$ decays in Fig. 13. The angle $\theta_A$ is the familiar Cabibbo angle measured in strange particle decay, $\theta = 13^o$, while the angle $\theta_B$ can be thought of as a Cabibbo angle for charmed particle decay. Both angles can be measured in $D^o$-decay via the ratios

$$\tan^2\theta_A = \frac{\Gamma(D^o \to K^-K^+)}{\Gamma(D^o \to K^-\pi^+)} \quad , \quad \tan^2\theta_B = \frac{\Gamma(D^o \to \pi^-\pi^+)}{\Gamma(D^o \to K^-\pi^+)}$$

Assuming $\theta_A = \theta_B$ and $SU_3$ invariance, one predicts

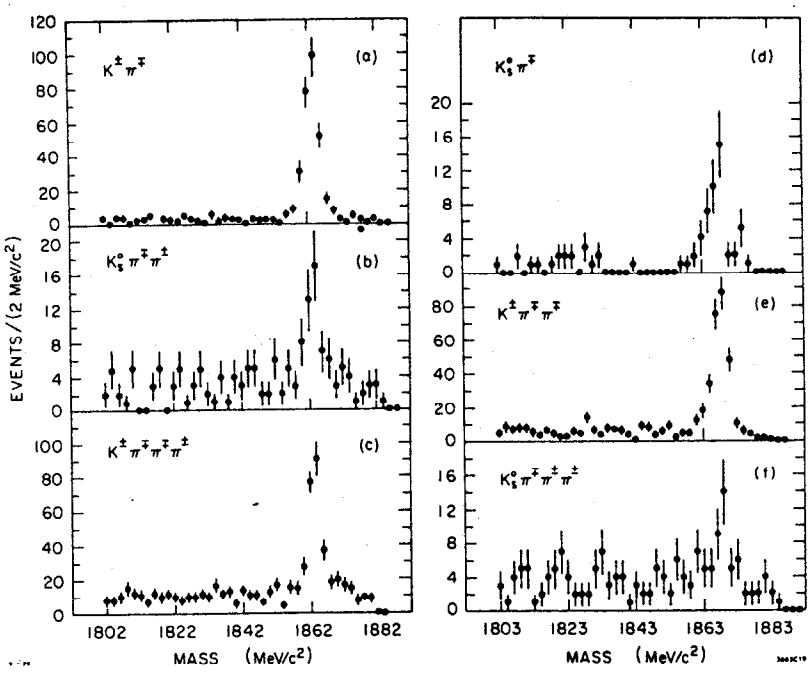


Fig. 11. Mass spectra for various decay modes of the $D^0(\bar{D}^0)$ (a-c), and the $D^+(D^-)$ meson (d-f).

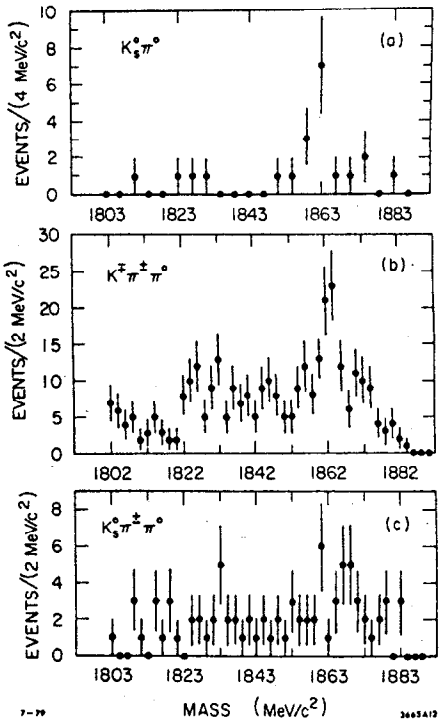


Fig. 12. Mass spectra for the decays (a) $D^0 \to K_S\pi^0$, (b) $D^0 \to K^-\pi^+\pi^0$ and (c) $D^+ \to K_S\pi^\pm\pi^0$.

Table II

D-Meson Branching Ratios

| Mode | # Events | ε | BR(%) | Mark I [27] BR(%) |
|---|---|---|---|---|
| $K^-\pi^+$ | 271 ± 17 | 0.436 | 2.8 ± 0.5 | 2.2 ± 0.6 |
| $\bar{K}^0\pi^0$ | 9 ± 3 | 0.021 | 2.1 ± 0.9 | |
| $\bar{K}^0\pi^+\pi^-$ | 39 ± 7 | 0.064 | 2.7 ± 0.7 | 4.0 ± 1.3 |
| $K^-\pi^+\pi^0$ | 37 ± 9 | 0.028 | 6.3 ± 2.2 | 12.0 ± 6.0 |
| $K^-\pi^+\pi^+\pi^-$ | 197 ± 16 | 0.133 | 6.7 ± 1.4 | 3.2 ± 1.1 |
| $\pi^+\pi^-$ | 9 ± 4 | 0.52 | 0.09 ± 0.04 | |
| $K^+K^-$ | 22 ± 5 | 0.37 | 0.31 ± 0.09 | |
| $\bar{K}^0\pi^+$ | 37 ± 7 | 0.10 | 2.1 ± 0.5 | 1.5 ± 0.6 |
| $K^-\pi^+\pi^+$ | 251 ± 17 | 0.29 | 5.2 ± 1.0 | 3.9 ± 1.0 |
| $\bar{K}^0\pi^+\pi^0$ | 9 ± 4 | 0.004 | 16.4 ± 9.5 | |
| $\bar{K}^0\pi^+\pi^+\pi^-$ | 22 ± 7 | 0.025 | 5.1 ± 2.0 | |
| $K^-\pi^+\pi^+\pi^+\pi^-$ | 5 ± 3.5 | 0.041 | < 2.0* | |
| $\bar{K}^0K^+$ | 6 ± 3 | 0.07 | 0.5 ± 0.27 | |

* 90% confidence limit.

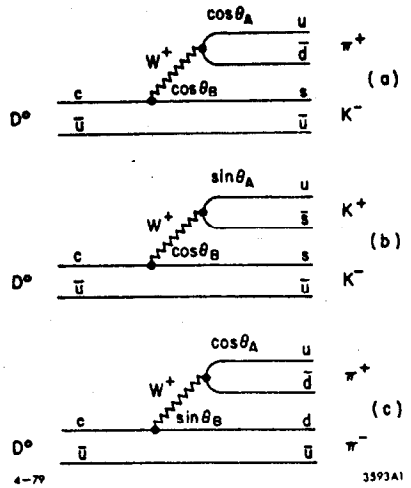


Fig. 13. Quark diagrams for $D^0$ decays to two charged particles.

$\tan^2\theta = 0.05$. Phase-space corrections raise the $\pi^-\pi^+$ by 7% and lower the $K^-K^+$ rate by 8%.

The two-body $D^o$ decays are identified in two steps. First, the pair of oppositely charged particles is required to have a total momentum of 288 ± 30 MeV/c, as expected for $D^o$'s produced in pairs at 3.771 GeV. Secondly, the two-body invariant mass spectra for the $\pi^-\pi^+$, $K^-\pi^+$, and $K^-K^+$ pairs identified by time-of-flight are evaluated, Fig. 14. Correctly identified decays appear near the $D^o$ mass, 1863 MeV/$c^2$, while pairs with one particle misidentified appear 120 MeV/$c^2$ below or above the $D^o$ mass. The dominant mode is $K^-\pi^+$ as expected, but there is a clear $K^-K^+$ signal, and excess of a few $\pi^+\pi^-$ events over the background. A maximum likelihood technique and Possion statistics is used to fit the data and estimate the backgrounds displayed as smooth curves in Fig. 14. The fit gives 235 ± 16 $K^-\pi^+$ decays, 22 ± 5 $K^-K^+$ decays, and 9.3 ± 3.9 $\pi^-\pi^+$ decays. The probability that the $\pi^-\pi^+$ signal is purely a statistical fluctuation of the background is $8 \times 10^{-3}$. Introducing the relative efficiencies gives $\Gamma(D^o \to \pi^+\pi^-)/\Gamma(D^o \to K^-\pi^+) = 0.033 \pm 0.015$ and $\Gamma(D^o \to K^-K^+)/\Gamma(D^o \to K^-\pi^+) = 0.113 \pm 0.030$, where the quoted errors include estimates of systematic errors that are dominated by the uncertainty in the background subtraction. A similar analysis has been carried out for $D^\pm$ decays. The measurement is limited by the poorer statistics; we obtain $\Gamma(D^+ \to \bar{K}^o K^+)/\Gamma(D^+ \to \bar{K}^o\pi^+) = 0.24 \pm 0.16$ and $\Gamma(D^+ \to \pi^o\pi^+)/\Gamma(D^+ \to \bar{K}^o\pi^+) < 0.2$. The results show that Cabibbo suppressed decays of charmed particles exist, and that they have the expected magnitude. For the $D^o$ decay, the $\pi^+\pi^-$ rate is lower than expected by one standard deviation, and the $K^+K^-$ rate is two standard deviations higher, which makes the interpretation difficult.[30]

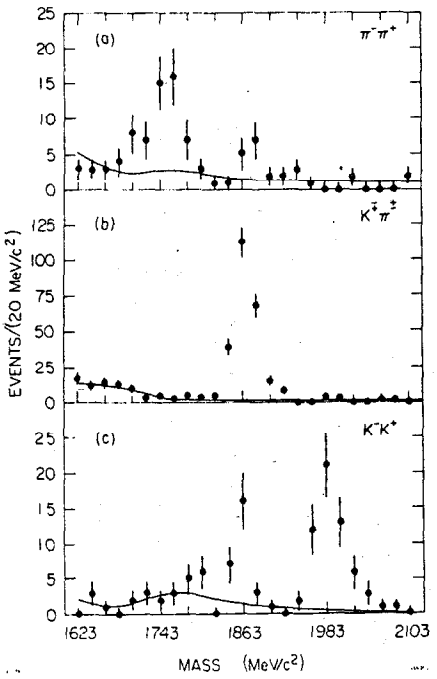


Fig. 14. Invariant mass of two particle combinations with momenta within 30 MeV/c of the expected $D^o$ momentum.

Inclusive Studies of D-Meson Decay

The simple nature of the $D\bar{D}$ final state in $\psi(3770)$ decays allows for inclusive studies of D decays. The $K^-\pi^+$ and $K^-\pi^+\pi^+\pi^-$ decay modes are used to tag $D^o\bar{D}^o$ events, the $K^-\pi^+\pi^+$ mode tags $D^+D^-$ events. These three decay modes have sufficiently large acceptance to be detected with reasonably small background. We observe 283 $K^-\pi^+$ decays with a background of 17 ± 2 events, 211 $K^-\pi^+\pi^+\pi^-$ decays including 31 ± 3 background events and 290 $K^-\pi^+\pi^+$ decays with 33 ± 2 background.

The observed charged multiplicity distributions corrected for background events, are shown in Fig. 15. No attempt has been made to identify neutral kaons so that a $K_s$ decaying to two charged pions will count as two charged particles. The observed multiplicity distribution can be related to the produced distribution by a Monte Carlo calculation simulating the $D\bar{D}^o$ and $D^+D^-$ production at 3.771 GeV (Fig. 15). While the neutral D meson decays primarily into two charged particles, the charged D meson decays with roughly equal rates to states with one and three charged particles. The average multiplicities are

$$\langle n_{ch} \rangle^o = 2.46 \pm 0.14$$

$$\langle n_{ch} \rangle^+ = 2.16 \pm 0.16$$

An earlier measurement by the LGW group[31] yielded $\langle n_{ch} \rangle = 2.3 \pm 0.3$. The numbers quoted include systematic errors due to uncertainties in the unfold and the background estimates. The statistical model[32] predicts somewhat higher charged multiplicities, typically 2.7.

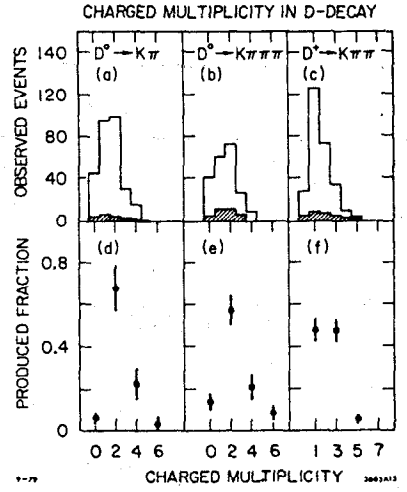


Fig. 15. Observed (a-c) and produced (d-f) multiplicity distributions for D-decays measured as recoils against $D^o \to K^-\pi^+$, $D^o \to K^-\pi^+\pi^+\pi^-$ and $D^+ \to K^-\pi^+\pi^+$. Errors are statistical only.

D-mesons are expected to decay dominantly into final states including one kaon. The kaon contents of D decays is measured by counting the charged and neutral kaons in the recoil system of tagged events. Charged kaons are identified by their time-of-flight, neutral kaons by their decays to two charged pions. The results, corrected for background events and the kaon detection efficiencies and branching ratios, are presented in Table III. We distinguish between the rates for kaons

Table III

Measurement of inclusive kaon and electron rates from decays of D-mesons. The rates corrected for double counting due to decays with more than one kaon are given in the last column.

| Mode | # of Tagged Events | Counts | Background | BR(%) Observed | BR(%) Corrected |
|---|---|---|---|---|---|
| $D^o \to K^-$ | 446 ± 23 | 111 | 5.1 ± 1.2 | 56.0 ± 5.6 | 51 ± 5 |
| $\to K^+$ | | 20 | 5.8 ± 1.3 | 7.9 ± 2.6 | |
| $\to K^o$ | | 15 | 5.1 ± 0.5 | 20.3 ± 8.5 | 17 ± 8 |
| $\to$ no K | | | | | 25 ± 11 |
| $D^+ \to K^-$ | 257 ± 18 | 21 | 2.2 ± 0.7 | 17.2 ± 4.1 | 16 ± 4 |
| $\to K^+$ | | 11 | 4.5 ± 1.6 | 5.6 ± 2.9 | |
| $\to K^o$ | | 13 | 3.5 ± 0.4 | 44.0 ± 15.0 | 38 ± 13 |
| $\to$ no K | | | | | 41 ± 16 |
| $D \to e^+$ | 775 ± 30 | 35 | | 9.8 ± 3.0 | |
| $D^+ \to e^+$ | 295 ± 18 | 38 | 15.0 ± 1.0 | 15.8 ± 5.3 | |
| $\to e^-$ | | 4 | 3.9 ± 0.5 | | |
| $D^o \to e^+$ | 480 ± 23 | 36 | 19.0 ± 1.0 | 5.2 ± 3.3 | |
| $\to e^-$ | | 19 | 12.0 ± 1.0 | | |

of different charge. 'Right-sign' kaons are of opposite charge compared to the kaon in the observed D-decays, 'wrong-sign' kaons have the same charge as the kaon in the observed D decay. The somewhat surprising result is the low branching fraction for the decay of the charged D to 'right-sign' charged kaons. Since in the GIM model, the $D^+$ decays to a $K^-$ and requires two additional charged particles to conserve charge, this decay is inhibited and one expects perhaps three times as many neutral kaons as charged kaons in $D^\pm$ decays.[32] Unfortunately, the low detection efficiency for $K_s$ prevents a sufficiently accurate measurement to test this hypothesis, but the data are consistent with an enhanced $K^o$ rate. If one corrects the observed rates for double counting due to contributions from Cabibbo suppressed decays containing more than one kaon, one can estimate the total branching fraction for D decays involving K mesons. If we assume that all decays containing 'wrong-sign' kaons are suppressed by a factor of $\tan^2\theta_c = 0.05$, we estimate that (25 ± 11)% of all neutral D-mesons and (41 ± 16)% of all charged D-mesons decay to final states not containing K mesons. These corrected rates are given in the last column of Table III. On the other hand, if we use the measured rates to 'wrong-sign' kaons, to derive a suppression factor of 0.15 ± 0.06, we obtain estimates of (31 ± 17)% and (44 ± 21)% for the decay to non-strange particles. In any case, the observed inclusive decay rates to kaons appear to be somewhat small compared to standard theoretical expectation, however, the errors are large due to low statistics. The results are in good agreement with a previous measurement.[31]

The sample of the tagged events at 3.771 GeV can be used to look for semi-leptonic decays of the second D. The results are presented in Table III. The principle problem in this measurement, apart from the limited statistics, is the background in the electron sample caused by the 6% misidentification of hadrons from decays. An upper limit on the error in the subtraction can be obtained from the signal of 'wrong-sign' electrons above the background, we obtain 0.1 ± 2.0 for the $D^+$ decay and 7 ± 4.5 for the $D^o$ decays. The observed leptonic branching ratio for $D^+$ exceeds that of the $D^o$ by two standard deviations. If we accept the basic prediction that $\Gamma(D^+ \to e^+) = \Gamma(D^o \to e^+)$, we can determine the ratio of the lifetimes from

$$\frac{\Gamma(D^o \to \text{all})}{\Gamma(D^+ \to \text{all})} = \frac{B(D^+ \to e^+)}{B(D^o \to e^+)} = \frac{\tau^+}{\tau^o}$$

i.e., the leptonic branching ratios are a measure of the relative particle lifetimes. The results obtained here are suggestive, but not precise enough to infer a difference in lifetimes. Such a difference is not totally unexpected.[34] Since the Cabibbo favored non-leptonic decays are $\Delta I_z = 1$ transitions, the $D^+$ decays mainly into I = 3/2 states, whereas the $D^o$ can decay to both I = 3/2 and I = 1/2 states. The hadronic rates should obey the inequality (up to $\tan^2\theta_c$)

$$0 \leq \frac{\Gamma(D^+ \to \bar{K} + \text{anything})}{\Gamma(D^o \to \bar{K} + \text{anything})} \leq 3 \quad .$$

## Limits on $F^{\pm}$ Meson Production

Compared to the detailed information that has been compiled on D-mesons, we have only a few hints concerning the $F^{\pm}$ meson, the $c\bar{s}$ bound state. All evidence comes from the DASP experiment at DORIS; it is based on inclusive $\eta$ production above 4.0 GeV and on 6 events at 4.4 GeV which can be fit to the hypothesis of either an $F\bar{F}^*$ or $F^*\bar{F}^*$ final state.[35] The decay $F^* \to F\gamma$ is observed. The mass is measured to be $2039 \pm 60$ MeV/$c^2$, where the error comes mostly from the ambiguity of the final state. The only explicity observed decay mode is $F^{\pm} \to \eta\pi^{\pm}$.

The Mark II group has analyzed hadronic events recorded above 4.0 GeV, in particular runs at 4.16 GeV and 4.42 GeV. Many different decay modes have been tried, but no convincing signal was found so far. In particular, inclusive $\eta$-production and the decay $F^{\pm} \to \eta\pi^{\pm}$ have been investigated. Figure 16a shows the invariant mass of two photons at 4.42 GeV. In order to reduce background from noise in the LA system we require $E_\gamma > 180$ MeV. Events in this plot are further selected by requiring that the momentum of one charged pion as well as the momentum of the two-photon system exceed 500 MeV/c. There is a dominant $\pi^0$ signal, but no evidence for the production of $\eta^0$ above the background from uncorrelated photons in the event. If we constrain all $2\gamma$ systems with an $m_{\gamma\gamma}$ in the region 450-650 MeV/$c^2$ to have the mass of the $\eta^0$, and then form the invariant $\eta\pi^{\pm}$ mass, we obtain the distributions in Fig. 16b,c. There is no signal around 2 GeV. Assuming a smooth background, we use these distributions to set upper limits on $F^{\pm}$ production. The detection efficiency is derived by Monte Carlo simulation for the process $e^+e^- \to F^+F^-$. The results are given in Table IV, together with limits for the decay $F^{\pm} \to \bar{K}^0K^{\pm}$ which were derived in a similar fashion. These limits are still compatible with the DASP measurement of $\sigma \cdot B(F^{\pm} \to \eta\pi^{\pm}) = 0.41 \pm 0.18$ nb.

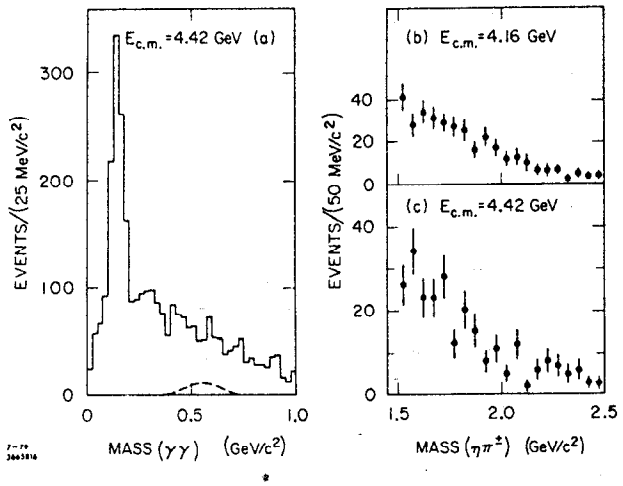


Fig. 16. Limits on inclusive F meson production. (a) Two photon invariant mass for multihadron final states at 4.16 GeV. The dashed line indicates the $\eta$ signal corresponding to the inclusive $\eta$ rate measured by DASP. Invariant $\eta\pi^{\pm}$ mass distributions at (b) 4.16 GeV, (c) 4.42 GeV.

Table IV

Upper Limits on Inclusive F Production
(Preliminary)

| Mode | Energy (GeV) | Efficiency (%) | Limit on (95% CL) $\sigma \times$ BR (nb) |
|---|---|---|---|
| $K^{\pm}\bar{K}^0$ | 4.16 | 5.8 | 0.13 |
| | 4.42 | 5.8 | 0.22 |
| $\pi^{\pm}\eta$ | 4.16 | 3.1 | 0.33 |
| | 4.42 | 4.5 | 0.26 |

## Inclusive Baryon Production

A measurement of the inclusive production of protons and $\Lambda$ hyperons, though important in its own right, is of particular interest as a test for charmed baryon production in $e^+e^-$ annihilation. Since charmed baryons are expected to decay to nucleons and hyperons, their production threshold should give rise to an increase in the number of protons and $\Lambda$ hyperons.

The analysis[45] is based on all multihadron events available outside the narrow resonances. TOF and momentum measurement are used to identify antiprotons up to 2 GeV/c. In this inclusive measurement protons are excluded, avoiding substantial beam-gas background. The $\bar{p}$ detection efficiency is estimated from a Monte Carlo model with antiprotons generated according to the invariant cross section $E/4\pi p^2 \cdot d\sigma/dp \sim e^{-bE}$, where E is the energy, p is the momentum of the $\bar{p}$, and b is an adjustable slope. A second nucleon and several pions are added according to the remaining phase space. After adjustment of the slope b and the mean particle multiplicity at each cm energy, this model reproduces the observed momentum spectra adequately. The detection efficiency for antiprotons averages 60%, increasing slowly with cm energy. Included in this efficiency are corrections for low momentum $\bar{p}$ which range out or interact or are not successfully tracked. The contamination by more copious lighter particles amounts to less than 15%.

$\Lambda$ and $\bar{\Lambda}$ hyperons are identified by $p\pi^-$ and $\bar{p}\pi^+$ decay modes. With a rms resolution of 3 MeV and a signal to background ratio of 4:1 or better. The detection efficiency is determined by the same Monte Carlo model as for antiprotons, it ranges from 10% at 3.67 GeV to 13% at 7.4 GeV.

The results, corrected for acceptance and the $\Lambda$ branching ratio, are presented in Fig. 17 in form of the ratio of the inclusive production cross section to the $\mu$-pair cross section as a function of cm energy, $R(p+\bar{p}) = 2 \cdot \sigma(\bar{p})/\sigma_{\mu\mu}$ and $R(\Lambda+\bar{\Lambda}) = [\sigma(\Lambda)+\sigma(\bar{\Lambda})]/\sigma_{\mu\mu}$. All errors are statistical; the estimated systematic errors of ±17% for p, and ±27% for $\Lambda$ are dominated by the uncertainties in the production process. The data confirm the rise in both $R(p+\bar{p})$ and $R(\Lambda+\bar{\Lambda})$ between 4.6 GeV and 5.2 GeV. The measurement of $R(p+\bar{p})$ is consistent with previous experiments,[36,37] the rates for $\Lambda$ are considerably higher than indicated by a previous measurement;[36] they are based on a cleaner signal and more detailed efficiency studies. The observed step sizes of $\Delta R(p+\bar{p}) = 0.30 \pm 0.05$ and $\Delta R(\Lambda+\bar{\Lambda}) = 0.10 \pm 0.03$ indicates that charmed baryon production

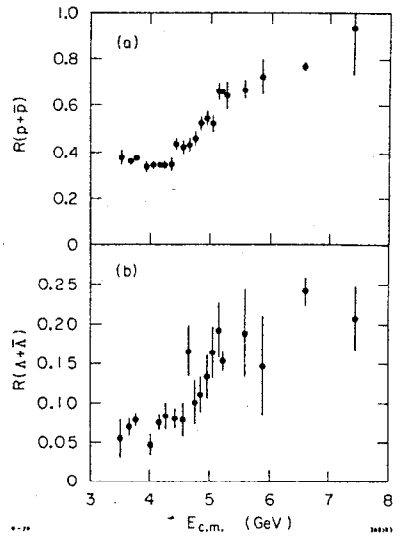


Fig. 17. Inclusive baryon production versus cm energy: (a) ratio of inclusive proton and antiproton to μ-pair production, $R(p+\bar{p}) = 2\sigma(\bar{p})/\sigma_{\mu\mu}$ and (b) inclusive Λ and $\bar{\Lambda}$ production to μ-pair production, $R(\Lambda+\bar{\Lambda}) = [\sigma(\Lambda)+\sigma(\bar{\Lambda})]/\sigma_{\mu\mu}$. Errors are statistical only.

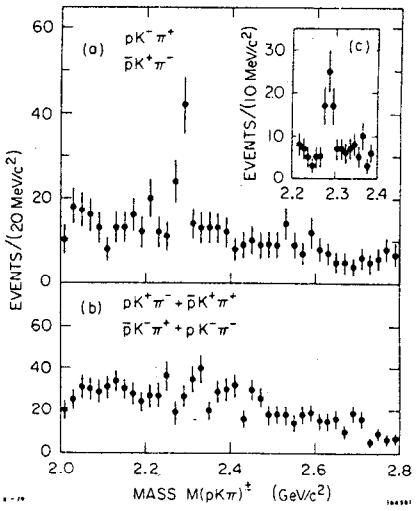


Fig. 18. Search for charmed baryon production. Invariant mass for (a) $pK^-\pi^+$ and $\bar{p}K^+\pi^-$, (b) $pK^+\pi^-$, $\bar{p}K^+\pi^+$, and $\bar{p}K^-\pi^+$, $pK^-\pi^-$, (c) same as (a) in 10 MeV/$c^2$ bins. The recoil mass is required to exceed 2.2 GeV/$c^2$.

amounts to roughly 20% of the total charm production, if the increase in cross section is due to charm threshold only. Furthermore, with the same assumption, the Λ/p ratio of (38 ± 10)% [38] indicates that weak decays of charmed baryons produce preferentially p, n or $\Sigma^{\pm}$ and not Λ or $\Sigma^0$.

## Observation of Charmed Baryon Decay

If the rise of the inclusive baryon cross section above 4.6 GeV is related to the threshold for the production of charmed baryons, their masses should be around 2.3 GeV. The most direct evidence for these states should come from the observation of narrow peaks in invariant mass spectra of two or more particles with baryon number one and at least one unit of strangeness. A search for such a signal[45] has been performed using all data available between 4.5 GeV and 6.0 GeV, totaling an integrated luminosity of 9150 $nb^{-1}$ (5150 $nb^{-1}$ at a fixed cm energy of 5.2 GeV). Charged kaons and nucleons are identified by the TOF system.

Figure 18 shows invariant mass distributions for pKπ combinations of various charge, strangeness, and baryon number having a recoil mass of more than 2.2 GeV/$c^2$. A narrow peak of 41 events over a background of 18 events is observed in the sum of the $pK^-\pi^+$ and $\bar{p}K^+\pi^-$ distributions, while $pK^-\pi^-$ and $\bar{p}K^-\pi^+$ combinations as well as their charge conjugates do not show any narrow enhancements. The signal represents at least a 5σ effect, it is observed with roughly equal strength in the $pK^-\pi^+$ and $\bar{p}K^+\pi^-$ state. The peak is centered at 2.285 ± 2 MeV/$c^2$, the observed width of 7 ± 1.5 MeV/$c^2$ agrees with the experimental resolution. This places an upper limit of 4 MeV/$c^2$ on the width of the state. The overall uncertainty in the absolute mass value is estimated to be less than 6 MeV/$c^2$. The uncertainty in the magnetic field was found to effect the mass by less than 2 MeV/$c^2$. A 20% error in the energy loss correction for protons and antiproton contributes at most 3 MeV/$c^2$. Furthermore, as an absolute calibration, the measured $K^0$ mass agrees with the world average to within 0.5 MeV/$c^2$. The $D^0$ mass varies by 3 MeV/$c^2$ in data sets recorded months apart at different energies. We assign ±4 MeV/$c^2$ as an upper limit for errors due to misalignment of the wire chambers and other geometric effects.

Other decay modes like $pK^0$, $\Lambda\pi^+$, $\Lambda\pi^+\pi^+\pi^-$ have been searched for in the same way as the $pK^-\pi^+$ mode. We observe 10 events above a background of 9 events in the $pK_s$ and $\bar{p}K_s$ channel in a 20 MeV/$c^2$ wide mass interval centered at 2290 MeV/c. No such signal is present in the $pK^-$ channel, though the detection efficiency is estimated to be five times larger than for $p\bar{K}^0$.

If the observed state is produced in pairs of equal mass then its energy should equal $E_b$, the energy of the beam, and its mass can be calculated as $M_x = (E_b^2 - p^2)^{1/2}$, where p is the measured momentum of the state. In Fig. 19 this mass $M_x$ is plotted for $pK^-\pi^+$, $pK_s$, $\Lambda\pi^+$ and their charged conjugates. From the pKπ data we conclude that (25 ± 10)% of the total of 41 events are associated with an equal mass recoil, while the rest of the events are recoiling against higher mass systems.[39] The other modes show a few events at 2.285 GeV/$c^2$, above a very small background. An analysis of the pKπ Dalitz plot taking into account the background under the peak yields resonance contributions of (12 ± 7)% for the $K^*(890)$ and (17 ± 7)% for $\Delta^{++}(1236)$.

The mass, the narrow width, the evidence for associated production, and the quantum numbers of the observed state suggest that the observed signal can be associated with the lowest mass charmed baryon, presumably the isosinglet $C_0^+$, often referred to as $\Lambda_c^+$.[40] Evidence for the existence of such a state was first observed in the BNL bubble chamber,[41] and has since been confirmed in photoproduction,[42] ν interactions,[43] and at the CERN ISR.[44] Most of these experiments report masses near 2.26 GeV/$c^2$, some with surprisingly small errors.

Using Monte Carlo estimates for the detection efficiency of (15 ± 3)% for the pKπ mode, the signal corresponds to a cross section times branching ratio of 0.032 ± 0.011 nb at 5.2 GeV. The inclusive $\bar{p}$ production

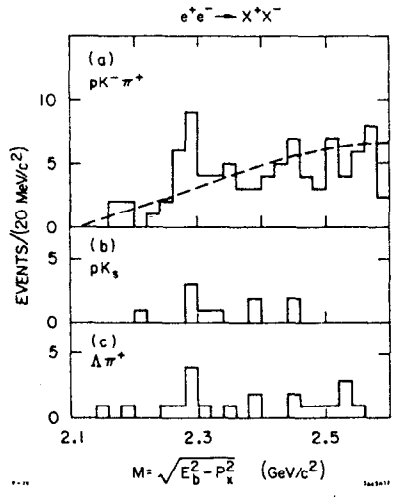


Fig. 19. Test on the reaction $e^+e^- \to X^+X^-$ where the particle $X^\pm$ decays to (a) $pK^-\pi^+$ or $\bar{p}K^+\pi^-$, (b) $pK_s$ or $\bar{p}K_s$ and (c) $\Lambda\pi^+$ or $\bar{\Lambda}\pi^-$. The dashed curve in (a) marks the estimated background.

rate can be used to derive an estimate of the absolute branching ratio for the observed $\bar{p}K^+\pi^-$ mode, under the following assumptions:

(1) The step $\Delta R(p) = 0.15 \pm 0.03$ is entirely due to the onset of pair production of charmed baryons.[46]

(2) All charmed baryons produced cascade down to the observed $C_0^+$ state.

(3) The $C_0^+$ decays to a proton (as opposed to a neutron) with a branching ratio of $0.6 \pm 0.1$.

Thus, we have

$$\sigma(e^+e^- \to C_0^+) = \frac{\Delta R(p)}{B(C_0^+ \to p)} \cdot \sigma_{\mu\mu}$$

and $\sigma(e^+e^- \to C_0^+ + \text{anything}) = 0.8 \pm 0.2$ nb. Consequently, the absolute branching ratio is

$$B(C_0^+ \to pK^-\pi^+) = \frac{\Gamma(C_0^+ \to pK^-\pi^+)}{\Gamma(C_0^+ \to \text{all})} = (2.0 \pm 0.8)\%$$

This rate is much smaller than the values assumed to estimate cross sections for associated production at the ISR.[44]

## Conclusions

Using large data samples recorded over the full energy range of the $e^+e^-$ storage ring SPEAR, the SLAC-LBL collaboration has exploited the improved resolution and particle identification of the Mark II detector to study particle production and decay in more detail than previous experiments:

(1) The more accurate measurements of $\tau^\pm$ branching ratios for the decays $\tau \to \rho\nu$, $\tau \to \pi\nu$, and $\tau \to \ell\nu\nu$ confirm the interpretation of the $\tau^\pm$ as a sequential heavy lepton and support the CVC hypothesis for the $\rho^\pm$ coupling.

(2) The measurement of the width of the $\eta'(958)$ marks the beginning of a new field of experimental physics: hadron production by scattering of photons on photons. This will certainly be explored at higher energies accessible by the new machines, PETRA[47] and PEP.

(3) Detailed studies of D-meson decay have not revealed any serious disagreement with the standard theoretical predictions, though there are several, possibly interesting effects at the level of 2-3 standard deviations. Considerably more data are needed to resolve any of these questions by a detailed comparison of branching ratios for different decay modes.

(4) The Mark II data do not confirm the existence of the $F^\pm$ meson, the upper limit of 0.26 nb for $\sigma(e^+e^- \to F^\pm)\, B(F^\pm \to \eta\pi^\pm)$ does not contradict the rate of $0.41 \pm 0.18$ nb observed by the DASP group. The search for other decay modes is, however, still in progress.

(5) There is now clear evidence for the production of charmed baryons in $e^+e^-$ annihilation above 5 GeV cm energy. The branching ratio of 2% for the decay $C_0^+ \to pK^-\pi^+$ is rather small.

In conclusion, in only 12 months of data taking, the Mark II has produced a large variety of results, their accuracy being mostly limited by statistics. Substantially more data will be needed to perform crucial tests of the theory of weak interactions of charmed particles with high accuracy, and to establish the $F^\pm$ meson and other charmed baryons. The answers to some of the open questions may improve our understanding of the weak hadronic currents in general.

## References


1. Members of the SLAC-LBL collaboration: G. S. Abrams, M. S. Alam, C. A. Blocker, A. M. Boyarski, M. Breidenbach, C. H. Broll, D. L. Burke, W. C. Carithers, W. Chinowsky, M. W. Coles, S. Cooper, B. Couchman, W. E. Dieterle, J. B. Dillon, J. Dorenbosch, J. M. Dorfan, M. W. Eaton, G. J. Feldman, H. G. Fischer, M. E. B. Franklin, G. Gidal, G. Goldhaber, G. Hanson, K. G. Hayes, T. Himel, D. G. Hitlin, R. J. Hollebeek, W. R. Innes, J. A. Jaros, P. Jenni, A. D. Johnson, J. A. Kadyk, A. J. Lankford, R. R. Larsen, D. Lüke, V. Lüth, J. F. Martin, R. E. Millikan, M. E. Nelson, C. Y. Pang, J. F. Patrick, M. L. Perl, B. Richter, J. J. Russell, D. L. Scharre, R. H. Schindler, R. F. Schwitters, S. R. Shannon, J. L. Siegrist, J. Strait, H. Taureg, V. I. Telnov, M. Tonutti, G. H. Trilling, E. N. Vella, R. A. Vidal, I. Videau, J. M. Weiss, H. Zaccone.
2. G. J. Feldman, Gordon Conference, August 1979.
3. J. M. Weiss, EPS Conference on High Energy Physics, Geneva, June 1979.
4. G. S. Abrams et al., to be published.
5. W. Davies-White et al., Nucl. Instrum. Methods 160, 227 (1979).
6. G. S. Abrams et al., IEEE Trans. on Nucl. Sci. NS-25, 309 (1978).
7. EGS, Electromagnetic Shower Program, R. L. Ford, W. R. Nelson, SLAC-Report 210 (1978).

8. M. Breidenbach et al., IEEE Trans. on Nucl. Sci. NS-25, 706 (1978); H. Brafman et al., IEEE Trans. on Nucl. Sci. NS-25, 692 (1978).

9. M. L. Perl et al., Phys. Rev. Lett. 35, 1489 (1975); M. L. Perl et al., Phys. Lett. 63B, 466 (1976).

10. W. Bacino et al., Phys. Rev. Lett. 42, 749 (1979).

11. G. Flügge, Zeitsch für Physik C1, 121 (1979); G. J. Feldman, Proceedings of the International Conference on High Energy Physics, Tokyo (1978), p. 777.

12. G. S. Abrams et al., submitted to Phys. Rev. Lett. (1979).

13. The notations $\tau^- \to \rho^- \nu_\tau$ and $\tau^- \to \ell^- \nu_\tau \bar{\nu}_\ell$ imply also the charged conjugate reactions $\tau^+ \to \ell^+ \bar{\nu}_\tau \nu_\ell$ and $\tau^+ \to \ell^+ \bar{\nu}_\tau \nu_\ell$.

14. G. J. Gilman and D. H. Miller, Phys. Rev. D17, 1846 (1978).

15. R. Brandelik et al., Zeitsch für Physik C1, 233 (1979).

16. F. E. Low, Phys. Rev. 120, 582 (1960); S. J. Brodsky, T. Kinoshita and H. Terazawa, Phys. Rev. Lett. 25, 972 (1970), and Phys. Rev. D4, 1532 (1971).

17. G. S. Abrams et al., Phys. Rev. Lett. 43, 477 (1979).

18. V. M. Budnev and I. F. Ginzberg, Phys. Lett. 37B, 320 (1971); V. N. Baier and V. S. Fadin, Nuovo Cimento Lett. 1, 481 (1971).

19. D. M. Binnie et al., Phys. Lett. 83B, 141 (1979).

20. H. Suura, T. F. Walsh and B-L. Young, Nuovo Cimento Lett. 4, 505 (1972); M. S. Chanowitz, Phys. Rev. Lett. 35, 977 (1975).

21. M. S. Chanowitz, LBL-9639 (1979).

22. P. A. Rapidis et al., Phys. Rev. Lett. 39, 526 (1977).

23. W. Bacino et al., Phys. Rev. Lett. 40, 671 (1978).

24. Cool and Marshak, Advances in Particle Physics, Vol. 2, p. 193 (1968).

25. A. M. Boyarski et al., Phys. Rev. Lett. 34, 1357 (1975); V. Lüth et al., Phys. Rev. Lett. 35, 1124 (1975).

26. E. Eichten et al., Phys. Rev. D17, 3090 (1978); T. Appelquist et al., Ann. Rev. Nucl. Sci. 29, 387 (1978).

27. I. Peruzzi et al., Phys. Rev. Lett. 39, 1301 (1977).

28. D. Fakirov, B. Stech, Nucl. Phys. B133, 315 (1978); N. Cabibbo and L. Maiani, Phys. Lett. 73B, 418 (1978).

29. N. Deshpande, M. Gronau and D. Sutherland, FERMILAB-PUB-79/70 (1979).

30. G. S. Abrams et al., Phys. Rev. Lett. 43, 481 (1979).

31. V. Vuillemin et al., Phys. Rev. Lett. 44, 1149 (1978).

32. C. Quigg and J. L. Rosner, Phys. Rev. D17, 239 (1978).

33. S. L. Glashow, J. Iliopoulos and L. Maiani, Phys. Rev. D2, 1285 (1970).

34. A. Pais and S. B. Treiman, Phys. Rev. D15, 2529 (1977).

35. R. Brandelik et al., Phys. Lett. 80B, 412 (1979).

36. M. Piccolo et al., Phys. Rev. Lett. 39, 1503 (1977).

37. R. Brandelik et al., Nucl. Phys. B148, 189 (1979).

38. This ratio has been corrected for protons from $\Lambda$ decays that are included in the inclusive proton rate.

39. The position of the peak for the recoil mass is an independent measure for the mass of the state, it agrees with the value obtained from the effective mass.

40. A. de Rujula, H. Georgi and S. L. Glashow, Phys. Rev. D12, 142 (1975).

41. E. G. Cazzoli et al., Phys. Rev. Lett. 34, 1125 (1975).

42. B. Knapp et al., Phys. Rev. Lett. 37, 882 (1976).

43. A. M. Cnops et al., Phys. Rev. Lett. 42, 197 (1979); C. Baltay et al., Phys. Rev. Lett. 42, 1721 (1979); C. Angelini et al., Phys. Lett. 80B, 428 (1979).

44. Contributions to the EPS Conference on High Energy Physics, Geneva 1979; D. Drijard et al., CERN-EP preprint (1979); K. L. Giboni et al., CERN-EP preprint (1979); P. Schlein et al., UCLA preprint (1979).

45. G. S. Abrams et al., submitted to Phys. Rev. Lett. (1979), SLAC-PUB-2406, and LBL-9855 (1979).

46. An upper limit of 0.5 nb (90% C.L.) on the production of charmed baryons in association with a charmed meson, $\bar{D}^0$ or $D^-$, had been obtained from a handscan of all events with a measured decay $D^0 \to K\pi$.

47. Ch. Berger, invited talk at this conference.